SUBCONTRACT TITLE: Innovative Characterization of Amorphous and Thin-Film Silicon for Improved Module Performance

SUBCONTRACT NO: NREL Subcontract ZXL-5-44205-11

QUARTERLY TECHNICAL STATUS REPORT: Phase III/Quarter 3
16 November 2007 to 15 April 2008

SUBMITTED TO: Bolko von Roedern
National Renewable Energy Laboratory

PRINCIPAL INVESTIGATOR: J. David Cohen, Department of Physics
University of Oregon, Eugene, OR 97403

This report covers the third quarter of Phase III for the period 16 November 2007 to 15 April 2008 of the Thin Film Partnership Subcontract ZXL-5-44205-11. Our Statement of Work calls for us to devote a portion of our effort to CIS thin-film photovoltaics. After the onset of our Subcontract with United Solar under their DOE/SAI contract to work on thin-film silicon based photovoltaics, we have shifted more of our effort under our NREL support to issues related to CIGS photovoltaics. Therefore, this Quarterly reports the latest results we have obtained in our studies of CIGS cells.

During this Quarter we have been applying junction capacitance methods to investigate the effects of Ga grading on a set of four $CuIn_{1-x}Ga_xSe_2$ (CIGS) sample devices frabricated by Miguel Contreras at the National Renewable Energy Laboratory (NREL). These samples were provided to Nanosolar as a reference set of devices. Jeroen van Duren at Nanosolar forwarded a portion of each one to my laboratory by for detailed study using our techniques.

One device was deposited with a uniform Ga depth profile (x=0.30), two were deposited so that the Ga fraction varied monotonically from near x=0.9 at the Mo back contact to either x=0.15 or x=0.25 at the junction interface, and the last device utilized a compositional variation close to NREL's optimal "v-shaped" bandgap grading scheme. Following deposition, SIMS measurements were carried out at NREL to provide a detailed spatial map of the Ga/(Ga+In) ratios in the CIGS absorbers. These profiles for the three compositionally graded devices are displayed in Figure 1 and the device performance parameters are listed in Table I.

Table I. Cell performance parameters for devices fabricated at NREL with different Ga/(Ga+In) grading profiles. Those grading profiles are displayed in Fig. 1.

Grading Type (Cell Number)	V_{OC} (volts)	J_{SC} (mA/cm^2)	FF (%)	Efficiency (%)
Uniform (26-2)	0.656	35.2	74.0	17.1
Monotonic A (28-2)	0.655	34.0	73.4	16.3
Monotonic B (30-4)	0.665	30.4	75.5	15.3
V-shaped (33-4)	0.636	31.7	74.8	15.1

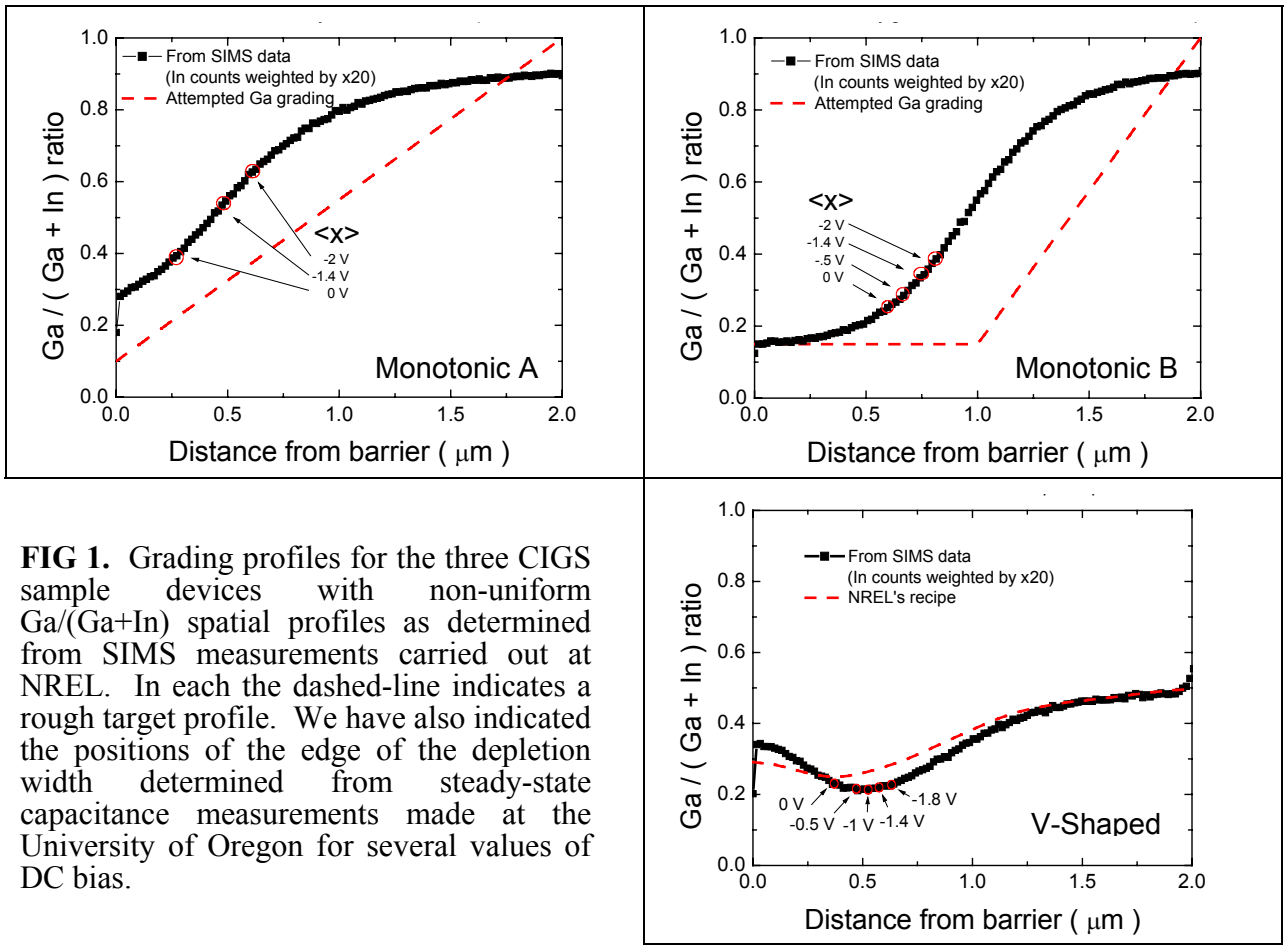

FIG 1. Grading profiles for the three CIGS sample devices with non-uniform Ga/(Ga+In) spatial profiles as determined from SIMS measurements carried out at NREL. In each the dashed-line indicates a rough target profile. We have also indicated the positions of the edge of the depletion width determined from steady-state capacitance measurements made at the University of Oregon for several values of DC bias.

One of the most revealing effects of Ga grading were obtained from our transient photocapacitance (TPC) and photocurrent (TPI) spectra. These measurements provided a spectral map of the optically induced release of carriers for photon energies from 0.6eV to 2eV. Comparing the two types of spectra enables one to distinguish majority from minority carrier processes. We also attempted to obtain additional spatial information by varying the applied DC bias to weight the spectral response to different regions relative to the barrier junction. The edge of the depletion region under different (steady-state) DC biases were estimated by the high frequency junction capacitance values and are indicated on the spatial profile maps shown in Fig. 1. However, the TPC and TPI measurements also involve the periodic application of voltage filling pulses (of 0.5 volts in the forward direction in each case). This causes the depletion widths to actually extend somewhat farther from the barrier junction than under constant DC bias. Thus, we are really sampling regions farther from the junction than the positions indicated in Fig. 1.

In Figs. 2,3, and 4 we display pairs of TPI and TPC spectra for 3 of the samples: the one with the uniform spatial profile, one of the monotonically profiled samples (A), and the v-shaped compositionally profiled sample, respectively. In all cases these spectra clearly identified the gap energy of the alloy composition nearest the barrier junction for each sample (1.0eV to 1.2eV depending on the sample). Very narrow bandtails (varying from 13 to 23meV) were observed indicating very low structural disorder.

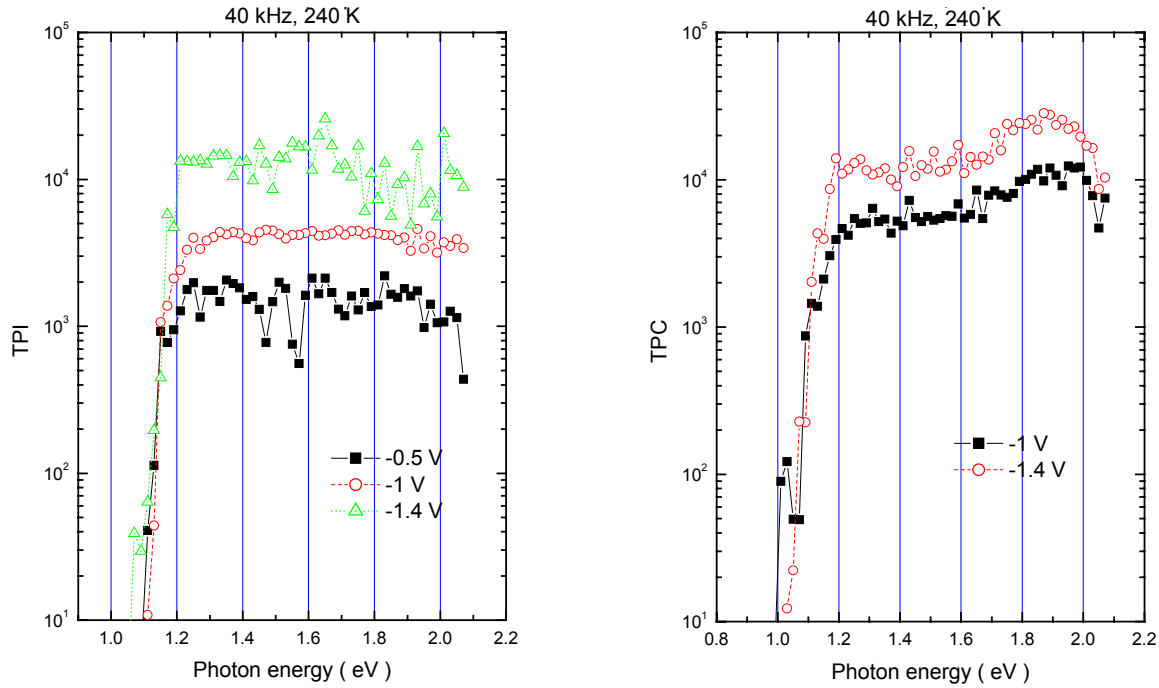

FIG. 2. Transient photocurrent (TPI) and transient photocapacitance (TPC) spectra obtained for the CIGS sample device with uniform grading at 240K at several values of reverse bias. Above the 1.2eV bandgap these spectra exhibit a fairly constant spectral response.

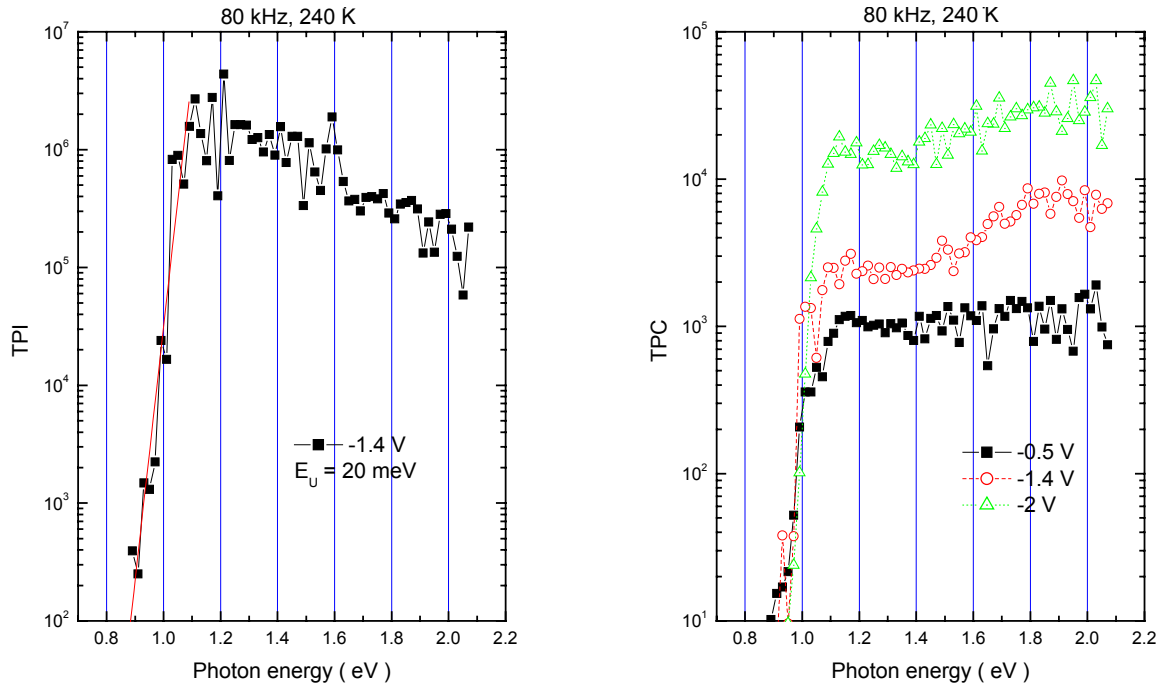

FIG. 3. Transient photocurrent (TPI) and transient photocapacitance (TPC) spectra obtained for the CIGS sample device with an increasing gallium fraction moving away from the junction (montonic B). Measurements were again made at 240K for several values of reverse bias. Note the larger variation with photon energy of the spectral response compared to the uniform case.

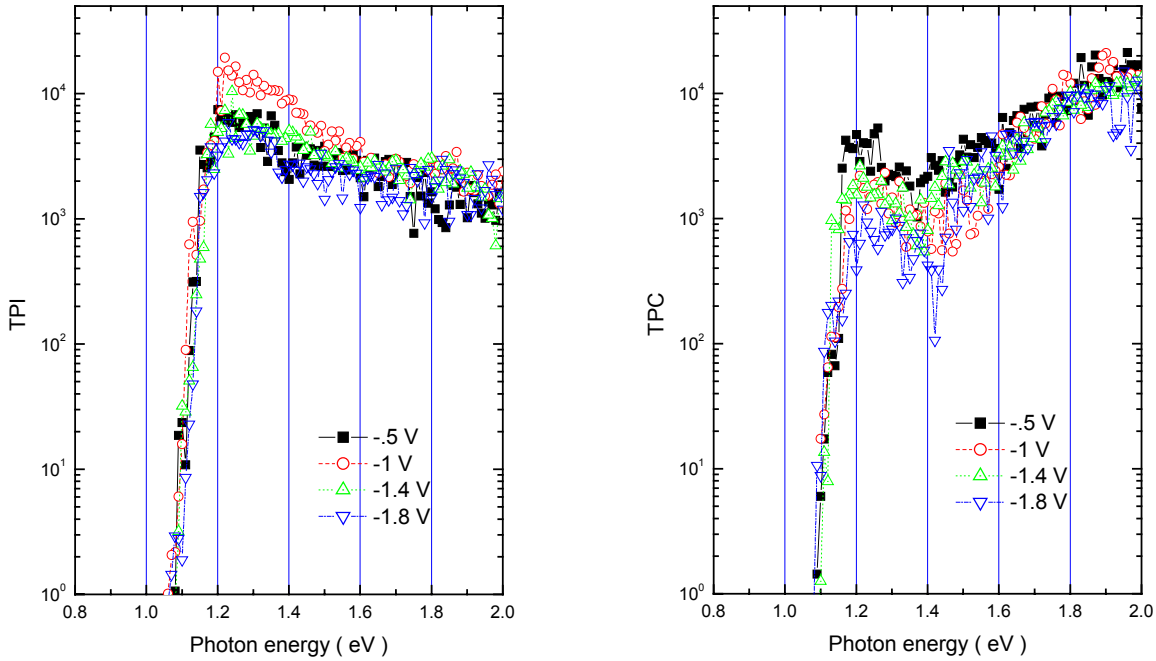

FIG. 4. TPI and TPC spectra for the sample device with a "V-shaped" Ga grading profile at 240K and different DC bias. Here the variation with photon energy above the bandgap is even more pronounced and reflects a substantial increase in minority carrier collection.

The TPI spectra for photon energies in Fig. 2(a) above the bandgap energy of 1.2eV is nearly constant in energy. This indeed reflects the spatial uniformity of the composition for that sample. The TPC spectra in Fig. 2(b) are also reasonably constant above 1.2eV, although they do increase by roughly a factor of 2 between 1.6eV and 1.9eV. The reason for this small increase is not yet clear. The fact that the TPI and TPC spectra exhibit slightly different spectral dependences can arise either because of varying degrees of minority vs. majority carrier collection *vs*. optical energy, or because the two measurements methods have different spatial sensitivities (majority carrier collection makes its largest contribution to the TPI signal near the barrier junction, but for TPC this contributes more strongly near the edge of the depletion region). In any case, the spectral variation above 1.2eV is not large.

The TPI spectra for both the samples with monotonically increasing bandgaps vs. distance from the junction are quite different, as illustrated in Fig. 3(a). Here we observe a maximum response at the bandgap corresponding to the alloy at the junction, following by a monotonically decreasing signal as the optical energy is increased further. This coincides with a slightly *increasing* TPC response for photon energies above 1.5eV as shown in Fig. 3(b). The latter partly reflects the increasing bandgap; however, the variation in the TPC/TPI ratio with photon energy probably also reflects the increased minority carrier (electron) collection in these samples. This agrees with the general understanding of how compositional grading improves overall cell performance.

Evidence for increased minority carrier collection is even stronger in the sample device incorporating the v-shaped Ga-grading, whose TPI and TPC spectra are displayed in Fig. 4. The types of variations of these signals with photon energy exhibited in Fig. 3 are now significantly

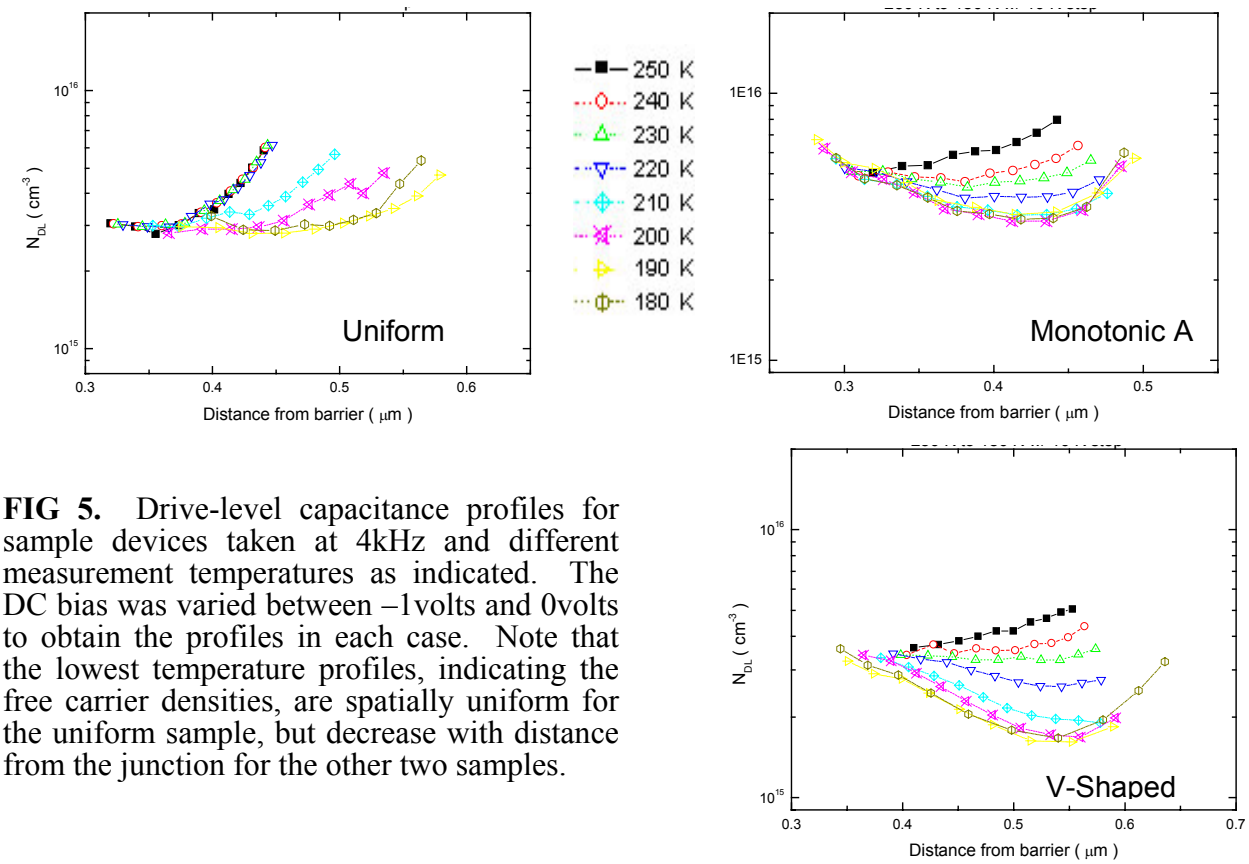

FIG 5. Drive-level capacitance profiles for sample devices taken at 4kHz and different measurement temperatures as indicated. The DC bias was varied between –1volts and 0volts to obtain the profiles in each case. Note that the lowest temperature profiles, indicating the free carrier densities, are spatially uniform for the uniform sample, but decrease with distance from the junction for the other two samples.

enhanced, particularly for photon energies 1.2 to 1.4eV. These spectra also exhibit a quite complex temperature dependent behavior whose details are still being analyzed. However, we believe that they can potentially provide a very complete picture of how compositional grading affects the minority collection in CIGS devices.

We also examined the spatial profiles of the free hole carrier densities and deep acceptor concentrations using drive-level capacitance profiling (DLCP). Results for the sample with the uniform compositional profile, a monotonically profiled sample, and the v-shaped compositionally profiled sample are displayed in Fig. 5. The lower temperature profiles reflect a free carrier density that is indeed uniform in the first case. However, the latter two instances display a marked *decrease* with distance from the barrier junction; that is, as the Ga fraction is increased. At the same time, the higher temperature profiles *increase* with distance. For the compositionally uniform sample this increase was unexpected since previously studied CIGS sample devices with uniform Ga fractions from IEC Delaware displayed more uniform DLCP profiles at higher temperature. However, in the compositionally varying samples this behavior may indicate an actual trend of decreasing free carriers and increasing deep acceptors with increasing Ga alloying. An alternate but intriguing second possibility is that it may be related to the behavior my laboratory has documented in the CIGS alloys under bias stress; namely, that there appears to be a metastable conversion of shallow acceptors into deep acceptors. In the case of compositionally profiled samples an effect similar to bias stressing may be occurring due to the variation in the energy gap which acts as an applied electric pseudo-field. Further studies will hopefully be able to examine this possibility in detail.